Essential Readings in Light Metals: Aluminum Reduction Technology.
Edited by Geoff Bearne, Marc Dupuis and Gary Tarcy.

FIELD STUDY OF THE ANODIC OVERVOLTAGE IN PREBAKED ANODE CELLS

Henrik Gudbrandsen[1], Nolan Richards[2], Sverre Rolseth[1] and Jomar Thonstad[3]

[1] SINTEF Materials Technology, Trondheim, Norway. [2] 117 Kingwood Dr., Florence, AL 35630, USA. [3] Dept. Materials Technology, Norwegian University and Technology, Trondheim, Norway.

Abstract

The anodic overvoltage in aluminum electrolysis represents 10 – 15% of the total cell voltage, and possible means of reducing the overvoltage should then be studied. In the present work the anodic overvoltage was measured in two prebake cells, 180 kA and 235 kA, the latter having some anodes with slots, and in one 145 kA HSS cell. A special reference electrode was used. At normal current densities the overvoltage varied from 0.72 V at 5 wt% Al_2O_3 to 0.86 V at 2 wt% . At comparable anodic current densities and alumina concentrations, the overvoltage for the anodes with one transverse 1.5 cm groove were 0.11 V less than for the conventional anodes. For the HSS cell the overvoltage was similar.

Introduction

The cell reaction in the Hall-Heroult process is,

$$½\ Al_2O_3 + ¾\ C = Al + ¾\ CO_2 \qquad (1)$$

which has a standard reversible emf of E° = - 1.186 V at 970 °C [1]. In order to make this reaction proceed, a voltage E_i, which is higher than the reversible emf is needed, and this extra voltage is named overvoltage,

$$\eta = E_i - |E^{rev}| \qquad (2)$$

E^{rev} is equal to E° at alumina saturation, otherwise its numerical value will be higher, according to the Nernst equation ($E^{rev} = E^o + RT/nF \ln a_{Al2O3}$), where a_{Al2O3} is the activity of alumina, the other terms having their usual meaning.

The objective of this field study was to measure the anodic overvoltage on industrial cells. In particular, measurements were made on anodes with a slot, to determine if such a slot facilitated the release of CO_2 gas, resulting in a time-averaged increase in the electroactive anodic surface area, and hence a decrease in the overpotential. The project was carried out on 180 kA and 235 kA prebake cells of Hydro Aluminium. Previous data obtained on 145 kA HSS cells of Reynolds Metals [2] are also reported.

Numerous studies of anodic overvoltage have been conducted in laboratory cells, while measurements in industrial cells are scarce [2,3]. The laboratory works have been reviewed in the 2nd and 3rd editions of the book "Aluminium Electrolysis. Fundamentals of the Hall-Heroult Process" [4,5].

Overvoltage data are normally presented as so-called Tafel plots,

$$\eta = a + b \log i \qquad (3)$$

where i is the current density and a and b are constants. The published Tafel data present a rather confusing picture, since the Tafel coefficients are fairly widely scattered [4,5]. One parameter that seems to influence the data, is the size and shape of the anode. For relatively large anodes facing downwards, the Tafel plots tend to curve upwards at above about 0.5 A cm^{-2}, compared to a straight Tafel line in a semi-logarithmic plot.

For rod-shaped vertical electrodes used in laboratory studies, straight Tafel lines have been observed up to above 1.0 A cm^{-2} [6]. The overvoltage has been found to decrease with increasing alumina content and to increase with increasing excess aluminum fluoride content. In a typical industrial type of melt containing 11 wt% excess AlF_3, saturated with alumina, the overvoltage at 0.8 A cm^{-2} was found to be 0.64 V [6]. For a melt with 3 wt% Al_2O_3 this would correspond to about 0.70 V.

Experimental

For the study on 180 kA point fed cells a fairly young cell (346 days old) was selected, which had a recent record of being quite stable. The cell was operating at a fairly low temperature, 953 to 941°C . There was a ledge estimated at 3 – 5 cm thick, sloping towards the heel of the anodes on which we made measurements, with about 6 cm clearance between the top of the ledge and the vertical side of the anode. The cell had 20 anodes with a replacement cycle of 28 days.

Knowledge of the geometric area of the anode was essential. A new anode had the dimensions, 151 x 70 x 50 cm high. Measurements on ten butts showed that the final dimensions after 28 days usage were (146.5 ± 2.2) x (63.9 ±3.5) x (13 ± 1) cm high. These numbers indicate a remarkable preservation of cross section and have implications about how much current was being conducted by the sidewalls.

These decreases in dimensions implied the following rates of carbon consumption,

From the horizontal surface,	1.32 cm/day
From the longitudinal vertical surfaces	0.08 ± 0.04 cm/day
From the transverse vertical surfaces	0.108 ± 0.05 cm/day

The ratio of these rates of carbon consumption is 1.0:0.06:0.08.

To obtain the horizontal geometric area of a particular anode, A_h, was straight-forward, knowing the dimensions of the new and spent anodes and accepting a linear decrease in that area with time,

$$A_h = 10570 - (1.8 \pm 0.9)(h)\ cm^2 \qquad (4)$$

where (h) is the number of hours that the anodes had been in place.

When combining estimates for the proportion of sidewall conduction in percent, c.f., by Taylor et al. [7], Zoric et al. [8] and this work (9.2% at 14 cm immersion) as a function of anode immersion, L, the following relationship for estimating sidewall area, A_s, was established,

$$f = (0.033 + 0.93\ L)\ \%\ (\pm 2\%) \qquad (5)$$

A_s= f [Σ(geometric sidewall areas for the period in the cell)] cm^2.

where f is a function reflecting the composite contribution from the longitudinal and transverse sidewalls derived from the ratios of the carbon consumption cited above. The R^2 value for the derivation of the factor f was 0.82 for 5 data points. As a further refinement, the geometric sidewall area over the 28-day cycle of an anode is given by {L [440 –0.0208(h)]}.

In the 235 kA cell the horizontal area of a new anode was 9800 cm^2. For this cell with an anode cycle of 28 days, the measurements of butts were (64.5 ±1.3) x (131.5 ±2.4) x (18.8 ± 1) cm. A graph of area versus time in the cycle gave the horizontal area of an anode during its cycle (slope, - 1.96 $cm^2\ hr^{-1}$).

The transverse and longitudinal sidewall effective areas were estimated to be contributing 6.6 and 10%, respectively, of the geometric areas. An equation for estimating the effective sidewall area, A_{side}, was;

$$A_{side} = L\ (31.6 - 2.31 \times 10^{-3} h),\ cm^2 \qquad (6)$$

Combining the duration in the cell with the stated proportions of the peripheral areas, less 210 cm^2 from the horizontal area of the slotted anodes, also prorated for time in the cell, yielded the geometric area for calculating apparent current density, i.

In some of the anodes on the 235 kA cell, slots were machined in three otherwise standard anodes. The slots were located along the mid-transverse axis of the anode, 1.5 cm wide, 13 cm deep at the outer and 16 cm deep at the inner (center aisle) vertical edges of the anode [9]. The initial anode dimensions were 140 x 70 x 60 cm high. These anodes were placed in a cell, 2545 days old, according to a schedule ensuring that measurements could be taken on anodes of variable age.

The equipment essential for the completion of these measurements included special reference electrodes, as shown in Figures 1 and 2. These comprised a boron nitride (BN) tube fitted into a stainless steel tube with a graphite sleeve covering the transition joint between the BN and the steel. A so-called Luggin capillary with a 1 mm hole was screwed into the wall of the BN tube, 3 cm from the bottom. The whole reference electrode was about 90 cm long. An alumina tube insulated tungsten rod passed through an electrically insulating plug at the top of the stainless steel tube to make contact with a pool of aluminum in the bottom. The aluminum did not reach up to the level of the Luggin capillary, an arm projecting 1.5 cm from the wall of the BN tube. Previously charged electrolyte was placed in the probe with a composition designed to be similar to that used in the cell. Reference electrodes of a somewhat similar design were previously used by Thonstad et al. [3].

From direct measurement of the depths of bath, metal and anode immersion for the specific anode, the probe could be placed with the Luggin capillary hard against the vertical surface just above the horizontal surface of the anode. This placement ensured that no ohmic potential drop through the bath was included in the reference electrode – anode carbon circuit. From past measurements in all of laboratory, pilot plant and industrial cells, this positioning captures the equipotential voltage for a finite,

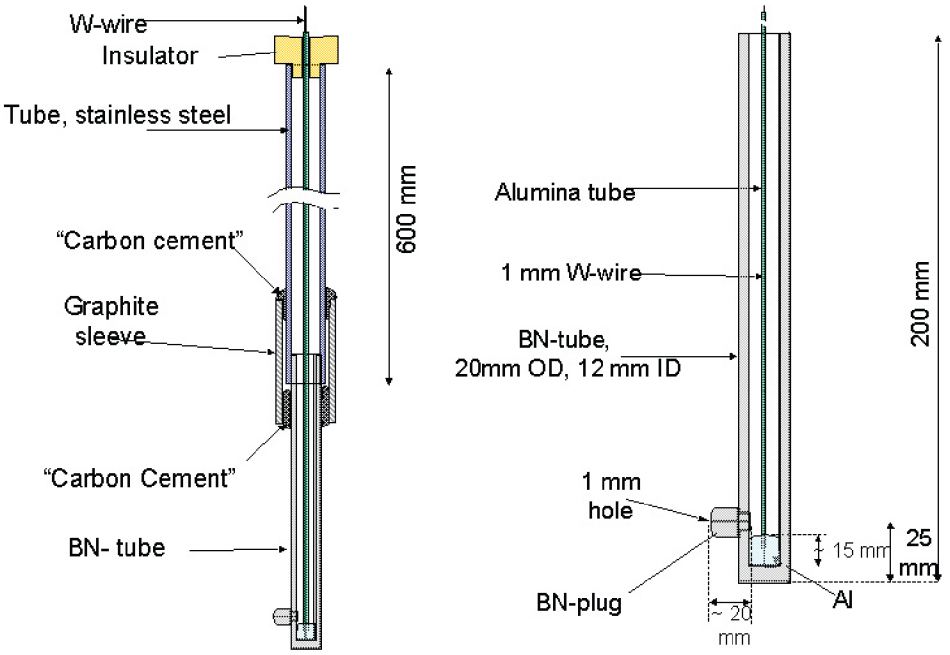

Figure 1. Reference electrode

dynamic zone, representative of the horizontal surface of the operating anode electrode, once it was in position. We used clamps insulated from the stubs of the anode and a specially constructed arm to lock the reference, once it was in position. The probe was located just off the centre line on the outer edge of the anode, as shown in Fig. 2.

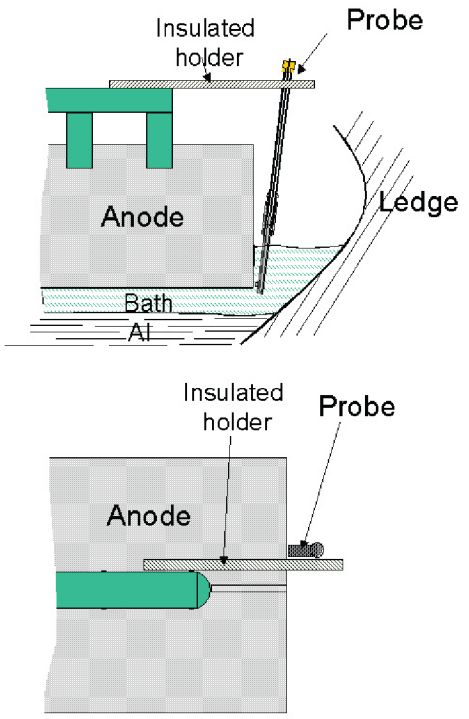

Figure 2. Location of reference probe, vertical and horizontal view.

The tungsten rod contacting the aluminum pool in the reference electrode, was the negative pole of a circuit through the anode to a steel stud implanted into the top of the anode, being the positive connection. The voltages for that circuit were captured on a data logger at the rate of five points per second. After acquisition of each set of data, they were downloaded to a computer.

Supporting equipment included a Halmar meter to measure the current in the anode, a thermocouple and meter to track the temperature beside the anode and tongs to take samples of bath, also in the close proximity of the subject anode.

The total cell voltage and line current obtained from the control panel of the cell, were noted and recorded frequently as an adjunct to keeping track of the operation of the cell. Parameters reflecting the state of the cell during five series of measurements on the 180 kA cell and the specific objectives of each, are summarized in Table 1, in which I is the line current and cd the current density. The excess AlF_3 was 8.5 wt%.

The anode overpotential was normally logged for at least 30 minutes, except when trending towards the anode effect and when manipulating the probe by hand along the vertical side of the anode to determine local current densities. The current density was otherwise varied by raising or lowering the anode under study, so that the total current passing through that anode varied. The temperature was measured and bath samples were taken from alongside the probe for subsequent analysis for alumina by LECO [10].

The voltage from the stud on the top of the anode to just above the bath line was measured. That voltage gradient per centimeter was used to obtain the additional potential drop from the lower contact point to the bottom edge or corner of the anode, where the probe was located. The voltage gradient through the carbon was reproducible at 1.8 mV/cm for the 180 kA cell and at 2.84 mV/cm for the 235 kA cell.

Results and Discussion

The apparent current density i, was derived by dividing the observed stem current (for which the variation is shown in column 3, Table 1, typically ± 400 A) by the calculated effective geometric area of the anode, determined by the procedure described above. The raw data from the data logger was taken in segments corresponding to intervals of the same or slightly different currents through the anode. The trace was never a simple line, because of the dynamics due to bubble formation and release, affecting the actual area of the anode. There was also a slower variation with a period of 30 – 40 seconds, possibly attributable to a wave motion in the aluminum cathode. The averaged plus/minus fluctuation in the particular section of the trace is listed in the fourth column. There were periodic peaks with amplitudes of 0.1 V.

Table I. Cell Parameters and Test Objectives for the 180 kA cell.

Series	Objective	Cell Volts	I, kA	Temp., °C
1	Track η on new anode	4.23 ± 0.02	180.2 ± 0.3	935 to 938
	Determine current density up side			
2	Measure normally	4.22	180.1	940
	Track η to anode effect	4.22 ⇒ 4.45	179.7	943⇒ 968 in 1 hr.
3	Monitor on recovery	4.60 ⇒ 4.26	179.7 ± 0.3	968⇒ 954 in 1 hr.
4	Obtain η at higher current density	4.23 ± 0.02	180.2 ± 0.2	953 - 952
5	Monitor for η and scan vertical side	4.28	180.5 ± 0.1	952

The primary data were corrected for the following voltages included in the electrical circuit tracked; E^o, the standard emf for reaction (1) at the appropriate temperature [1], a small correction due to the differential activity of alumina (about 28 mV), the IR voltage drop from the positive connection on the anode to the bottom of the immersed anode and the thermoelectric force from the tungsten – carbon thermocouple included in the circuit. (This was known from past work to be 5 mV).

Excluding those values of Al_2O_3 concentrations when the point feeders were turned off to achieve an anode effect, the average concentration during the campaign on the 180 kA cell was 5.7 wt%, which was higher than expected for a point-fed cell with automated control.

As mentioned above, one expects normally to obtain straight Tafel lines in a semilogarithmic plot, according to Eqn. (3). However, for large anodes facing downwards, one often experiences that the curves in Tafel plots tend to bend upwards, and in such cases a linear plot of overvoltage versus current may be more appropriate. The following dependencies were established for the data for the 180 kA cell, excluding the η's proceeding to the anode effect;

$$\eta = 0.34 + 0.52\ i\ (\pm 0.03)\ V \qquad (7)$$

For $0.6 < i < 1.3$

In a series when the change in η was tracked to anode effect at constant current density, η increased exponentially from 0.72 V at 5.3% to 0.88 V at 2.2% Al_2O_3. The plot of η versus wt% Al_2O_3 gave the coefficients, $[d\eta/dAl_2O_3]$. These were,

Alumina wt.%	5.5	4.5	3.5	2.5
$[d\eta/d\ Al_2O_3]$	0.015	0.025	0.040	0.073
$[d\eta/d\ Al_2O_3]$ for 145 kA HSS [2]		0.052	0.062	0.100

Using the coefficient for 5.5%, the η's obtained experimentally were all corrected to the common alumina concentration, 5.5%, and subjected to a numerical correlation by regression analysis, which resulted in,

$$\eta = 0.39 + 0.45\ i,\ (\pm 0.035)\ V,\ R^2 = 0.892 \qquad (8)$$

The results for traversing the Luggin capillary up and down the vertical side of an anode whilst in contact with the carbon, and the current densities inferred from a linear extrapolation of the η - i relationship, e.g. Eq. (7), are summarized in Table II, in the fourth column. The current density decreased at a rate of 0.048 to 0.067 A cm^{-2}/cm up the side of anodes, depending on the depth of immersion (13 – 10 cm). The plots were slightly curved. This compares favorably with that calculated from models [8].

From these field measurements, it is now possible to derive the anode overvoltage for a prebake cell as a function of both current density in the range of 0.65 to 1.25 A cm^{-2} and with varying alumina concentration. Calculations can also be made for the current densities on the sides of the anodes, depending upon the selection of bath depth and interelectrode distance and the distance to the ledge or to a neighboring anode.

Table II. Current Densities on the Vertical Sides of an Anode of the 180 kA cells as a Function of Distance up the Vertical Side.

Immersion cm	Distance from bottom, cm	Obsd. η V	Current Density, A/cm^2
13	0	0.71 ± 0.03	0.72 ±0.04
	2.5 ±0.5	0.63 ± 0.03	0.55
	5 ±0.5	0.60 ± 0.03	0.50 ±0.03
	9 ±0.5	0.60 ± 0.03	0.28
10	0	0.81 ± 0.06	0.9 ± 0.02
	2.5 ±0.5	0.65 ±0.02	0.6
	9	0.47 ±0.02	0.24 ± 0.03
	0	0.78 ±0.04	0.9
	6.5 ±0.5	0.54 ±0.02	0.38
	9.5	0.42 ±0.04	0.14 ±0.08

The superheat was measured with an Electro-Nite probe [11,12] on two occasions, about 1° and 4.2 °C. That calculated from analytical data and phase diagrams [13] was 4 ± 0.3° for 3.5% Al_2O_3 (actually, 3% in the cell), so the agreement on that parameter was good.

The raw data printed out from the logging, were interpreted for sequential time intervals appropriate to the variation or stability of the anode current. It included the amplitude of fluctuation in the overpotential due to the generation and release of gas bubbles, impacting the actual anodic surface area.

The anode overvoltages for the 180 kA cell were higher than would be predicted by some laboratory data, (e.g., $\eta = 0.47 + 0.33 \log i$ [14]). This is largely due to the screening by the anode gas so that the actual, instantaneous current density is higher than the apparent, and therefore, the relevant number for i to insert in the Tafel equation is not known.

For the 180 kA cell as well as the 235 kA cell, with alumina at 5.5 wt%, the anode overvoltages are given by Eqn. (8). At lower concentrations of alumina, the anode overvoltage increased at constant current density, and hence, the appropriate coefficient must be applied to obtain η's relevant to the specific range of alumina concentration used in a potline. The anode overvoltage increased from 0.72 V at 5.5 wt% Al_2O_3 to 0.88 V at 2.2 wt%, while the cell voltage increased by 0.19 V.

The nominal current density for the 180 kA cell was about 0.81 Acm^{-2} and for the 235 kA cell it was 0.80 Acm^{-2}. The current density was varied from 0.66 to 1 A cm^{-2} by raising or lowering the particular anode under study. This was done on both cells.

For the 235 kA cell the following relationships emerged:

For slotted anodes,

$$\text{by regression; } \eta = 0.17 + 0.639\ i,\ R^2 = 0.76, \qquad (9)$$

ave. devn. 0.06 V.

For standard anodes,

$$\text{by regression, } \eta = 0.145 + 0.786\ i,\ R^2 = 0.98, \qquad (10)$$

ave. devn. 0.018 V. with $0.5 < i < 1.20$ A cm^{-2}.

These results are presented graphically in Figure 3.

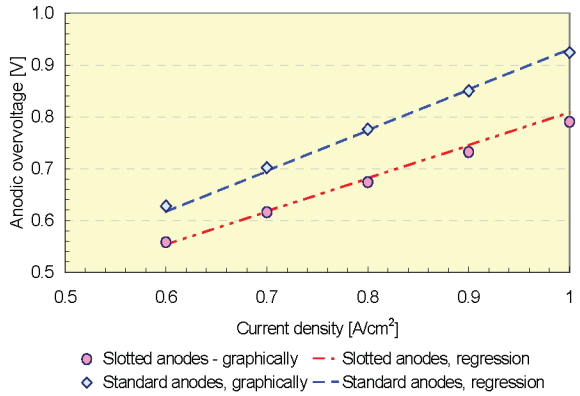

Figure 3. Anode overvoltage as a function of current density on a 235 kA cell.

In case that the line current could have been lowered so that the overvoltage could be recorded at current densities in the range 0.1 to 0.4 A cm^{-2}, a Tafel relationship (Eq. (3)) would probably have emerged.

From these results, the anode overvoltages for single slotted and standard (140 x 70 cm) anodes in a 235 kA cell can be compared in Table III.

Table III. Comparison of Anode Overvoltages for Anodes in the 235 kA cell, with and without a Single Slot, with Alumina in the Range 2 – 3 wt%.

Apparent cd, A cm^{-2}	0.6	0.8	0.9	1.0	1.1
Standard anode, η, V	0.63	0.78	0.87	0.92	1.0
Slotted anode, η, V	0.56	0.67	0.73	0.79	0.85
Difference, V	0.07	0.11	0.14	0.13	0.15
Difference by regress.	0.07	0.09	0.10	0.12	0.14

Consequently, the field study shows that the anodic overvoltage was decreased for the anodes with a groove, confirming by implication, that the slot facilitates the emission of the gas bubbles, thereby increasing the time averaged effective area of the anode. This means that the screening effect of the bubbles is reduced compared with that of standard anodes [15].

For the 235 kA cell with 30 anodes, at any one time only near 29 anodes are carrying nominal current, at the current density of [8050/9325 =] 0.86 A cm^{-2}, derived for the anode at mid-cycle. The grooved anodes would be operating at 0.11 ± 0.02 V lower than the standard. However, since the grooves are only minimum 13 cm deep and the anode consumption is about 1.47 cm/day, the slots would be effective for only 8.8 days. Employing a full set of slotted anodes then, 30% of that reduction in voltage should be attainable for the total cell voltage, i.e., 33 mV. If it could be discovered and confirmed that the enhanced release of gas bubbles also meant that the extension of the gas bubbles from the horizontal surface downwards toward the metal pad was less than the perceived average of 5–7 mm, then an additional few tens of millivolts, say 30 mV, might be conserved.

The anodic overvoltage increases with decreasing alumina concentration, a dependency that has been confirmed in both laboratory and plant studies [3,4,14,16]. From the work on the 180 kA cell, where the variation in Al_2O_3 was part of the parametric study, at the levels of concentration encountered in that study, the dependence of η for "standard" anodes was 0.073 V/wt.% Al_2O_3 at 2.5 wt%. That implies that with alumina varying from 2 to 3 wt.% at constant current density, the value of η is decreasing by about 70 mV.

In previous measurements of anode overvoltage on a 145 kA HSS cell, it was found [2],

$$\eta = 0.045 + 0.755 \cdot i, \text{ V} \qquad (10)$$

and the relationship between η and i was similarly linear over the range 0.55 - 0.9 A cm^{-2} . The higher coefficient, 0.75 per decade, for this cell, at current density 0.8 Acm^{-2}, is attributable to the greater screening, i.e., lower actual surface area of the much larger, single anode. A graphical comparison between Eq. (10) and Eq (8) is shown in Figure 4.

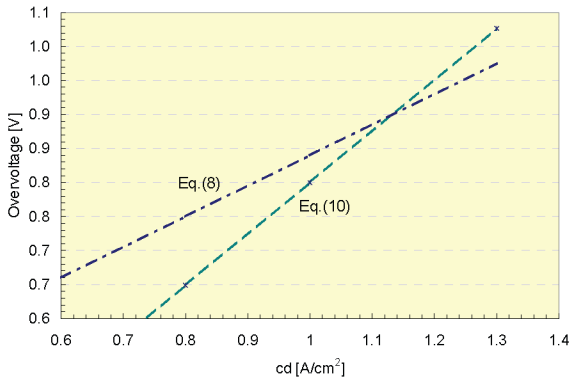

Figure 4. Comparison on overvoltage measurements on industrial cells. 145 kA HSS cell (Eq. (10) and 180 kA PB cell (Eq.(8)).

Thonstad et al. [3] carried out similar measurements on 75 kA VSS Soderberg cells and fitted the data to a Tafel equation (3), with a = 0.6 – 0.7 and b = 0.26, for the range 3.3 – 6.5 wt% Al_2O_3.

Conclusion

The anodic overvoltage on prebake anodes was found to vary in the range 0.86 V to 0.72 V for alumina contents ranging from 2.2 to 5.5 wt% Al_2O_3.

The overvoltage decreases with increasing alumina content.

Slots in the anodes effect a decrease in the anodic overvoltage. When applied to all the anodes in a cell such as the 235 kA, the projected decrease in total cell voltage would be 0.03 V. Possibly the interelectrode distance might be decreased slightly due to the enhanced release of bubbles.

Acknowledgement

Financial support from The Norwegian Research Council and from the Norwegian aluminum industry is gratefully acknowledged. The authors would also like to thank Kåre Vee at Hydro Aluminium Technology Center Årdal, for financial support of the final series of measurements. The invaluable assistance from plant personnel, viz., Elin Haugland, Trond Store, Jan Haugen and Ola Jakobsen, made this investigation possible.

References

1. M.W. Chase et al.,JANAF Thermochemical Data, 3nd ed.Nat. Bureau of Standards, Washington, 1975.

2. J.S. Berry and N. E. Richards, "Selected Properties of the San Patricio Cell", Reynolds Metals Report, Apr. 25, 1966.

3. J. Thonstad, A. Solbu and A. Larsen, "The decomposition voltage of aluminium reduction cells. The influence of the alumina content in the bath", J. Appl. Electrochem. 1, 261-268 (1971).

4. K. Grjotheim, C. Krohn, M. Malinovsky, K. Matiasovsky and J. Thonstad, "Aluminium Electrolysis. Fundamentals of the Hall-Heroult Process", 2nd ed., Aluminium-Verlag, Dusseldorf, 1982.

5. J. Thonstad, P. Fellner, G.M. Haarberg, J. Hives, H. Kvande and Å. Sterten, "Aluminium Electrolysis. Fundamentals of the Hall-Heroult Process", 3rd ed., Aluminium-Verlag, Dusseldorf, 2001.

6. Kisza, J. Kazmierczak, J. Thonstad, T. Eidet and J. Hives, "The Kinetics and Mechanism of the Electrode Reactions in Aluminium Electrolysis", Light Metals 1999, 423-429.

7. M.P. Taylor, B.J. Welch and M.S. Sullivan, Chemeca 83, Proc. 11th Australasian Chem. Eng. Conf., Brisbane, 1985, 437.

8. J. Zoric, J. Thonstad and T. Haarberg, The influence of current distribution by the initial shape and position of an anode and by the curvature of the aluminium in prebake aluminium cells", Light Metals 1998, 445-453.

9. B.P. Moxnes, B.E. Aga and J.H. Skaar, "How to Obtain Open Feeder Holes by Installing Anodes with Tracks", Light Metals 1998, 247-255.

10. G.P. Tarcy, Sverre Rolseth and Jomar Thonstad, "Systematic Alumina Measurement Errors and their Significance in the Liquidus Enigma", Light Metals 1993, s.227-232.

11. P. Verstreken, S. Benninghoff, "Bath and liquidus temperature sensor for molten salts", Light Metals 1996, 437-444.

12. S. Rolseth, P. Verstreken, and O. Kobbeltvedt, "Liquidus temperature determination in molten salts", Light Metals 1998, 359-366.

13. E. Skybakmoen, A. Solheim and A. Sterten, "Phase Diagram Data in the System Na_3AlF_6 –Li_3AlF_6 – AlF_3 – Al_2O_3. Part 1", Light Metals 1990, 317-324.

14. B.J. Welch and N.E. Richards, Extraction Metallurgy of Aluminum, Vol. 2, Interscience, New York, 1963, 15-30.

15. N. E. Richards, "The Dynamics of Components of the Anodic Overvoltage in the Alumina Reduction Cell", Light Metals, 1998, 521-529.

16. N.E. Richards and J.S. Berry, "Observations of Frequencies in anodic Currents", Reynolds Metals Company Report, Apr. 27, 1972.